Chaos, Solitons and Fractals 150 (2021) 111056

Contents lists available at ScienceDirect

Chaos, Solitons and Fractals

Nonlinear Science, and Nonequilibrium and Complex Phenomena

journal homepage: www.elsevier.com/locate/chaos

Classification based on dynamic mode decomposition applied to brain recognition of context

S. Martínez[a,*], A. Silva[b,e], D. García-Violini[c], J. Piriz[d,e], M. Belluscio[b,e], R. Sánchez-Peña[a,e]

[a] Instituto Tecnológico de Buenos Aires (ITBA), Av. Eduardo Madero 399, CABA C1106, Argentina
[b] IFIBIO Houssay, Grupo de Neurociencia de Sistemas, Facultad de Medicina, Universidad de Buenos Aires, Argentina
[c] Departamento de Ciencia y Tecnología, Universidad Nacional de Quilmes, Bernal, Argentina
[d] IFIBYNE, Facultad de Ciencias Exactas y Naturales, Universidad de Buenos Aires, Argentina
[e] Consejo Nacional de Investigaciones Científicas y Técnicas (CONICET), Buenos Aires, Argentina

ARTICLE INFO

Article history:
Received 31 December 2020
Revised 10 March 2021
Accepted 8 May 2021
Available online 30 June 2021

Keywords:
Context exploration
Local field potential
Dynamical model
Dynamic mode decomposition

ABSTRACT

Local Field Potentials (LFPs) are easy to access electrical signals of the brain that represent the summation in the extracellular space, of currents originated within the neurons. As such, LFPs could contain information about ongoing computations in neuronal circuits and could potentially be used to design brain machine interface algorithms. However how brain computations could be decoded from LFPs is not clear. Within this context, a methodology for signal classification is proposed in this study, particularly based on the Dynamic Mode Decomposition method, in conjunction with binary clustering routines based on supervised learning. Note that, although the classification methodology is presented here in the context of a biological problem, it can be applied to a broad range of applications. Then, as a case-study, the proposed method is validated with the classification of LFP-based brain cognitive states. All the analysis, signals, and results shown in this study consider real data measured in the hippocampus, in rats performing exploration tasks. Consequently, it is shown that, using the measured LFP, the method infers which context was the animal exploring. Thus, evidence on the spatial codification in LFP signals is consequently provided, which still is an open question in neuroscience.

1. Introduction

Understanding the human brain is probably the last frontier of biological sciences. Our brain works by the organized activity of billions of neurons that express through electrical signals. At the extracellular space the correlate of those neuron-generated currents originates spatial and temporal voltage gradients that could be measured and used to study brain functions. The local field potential (LFP), which can be mathematically described as a quasi-periodic stochastic process [1], is the sum of all trans-membrane cell currents within a volume. In this way, the LFP is the result of a neuronal population activity that could be used as a read-out of local computations. Two relevant aspects of the LFP signal should be highlighted. Firstly, LFP, like EEG, is an easy to access and low dimensional signal and, secondly, since LFP represents the spatial summation of currents from a vast number of sources, understanding its relationship with neuronal activity is highly complex. This complexity is ubiquitous in computational neuroscience, due to multi-scale physical interactions and to the high connectivity of the networks responsible of the brain dynamics, which in turn have a variable architecture. Due to the intrinsic brain features, it is not straightforward to obtain models via classical physical approaches as, for example, energy and mass balances. There are a variety of modeling strategies and model identification techniques that use data coming from real systems [2]. These data can be interpreted as knowledge about certain variables related to the states of the system. The methods based on time series obtained from measurements or simulations that aim to infer the evolution of a dynamical system to, for example forecast or control, are within the scope of data-driven methods [3]. A subclass of these methods, are referred to as equation-free methods, and in that approach the dynamical equations may be unknown. Their goal is to approximate the systems under study with a variety of numerical, algorithmic, and multi-scale sampling strategies. In this regard, the obtained representations circumvent the derivation of explicit equations that may exist, but are not available in closed-form.

Generally, a widespread way to understand complex networks is to apply modal decomposition techniques to data, whether considering spatial or temporal correlations, as well as analytic or

* Corresponding author.
E-mail address: sebamartinez2@gmail.com (S. Martínez).

https://doi.org/10.1016/j.chaos.2021.111056
0960-0779/

empirical kernels. These methods allow, for example, source separation like in Independent Component Analysis (ICA) or data compression, performed by Principal Components Analysis (PCA). But perhaps, the most widely used tools to analyze brain signals are related to Fourier decomposition, such as the Fast Fourier Transform (FFT) or the Power Spectral Density (PSD). For example, different cognitive states are characterized by their spectral content, e.g., the θ rhythm (typical in exploration tasks) shows an oscillation frequency in the 8 Hz–12 Hz band [4].

The Dynamic Mode Decomposition (DMD) method can be interpreted as a combination of dimensionality reduction techniques, such as PCA, along with time-domain Fourier analysis. The main advantage of DMD is its dynamical approach, in which, the data under study are assumed to be observations from an underlying dynamical system and does not rely on explicit modeling equations. This characteristic is particularly useful to study the complex brain signals, since the dynamic variation can occur simultaneously spatio-temporally.

There are several examples of DMD applications in the neuroscience field, in particular the following works are related, either in the biological approach, or for having inspired the analytical methodology [5,6]. The first one applies the DMD method to identify coherent patterns in large scale neural recordings, particularly focusing on episodes related to spindles. In the second one, DMD is applied to detect seizures in electroencephalograms (EEG)

Based on the previous arguments, a method to extract information concerning neuronal activity from LFP recordings and test its validity in a well-understood example of neuronal encoding, entails an important application.

Here we use as a model the well-studied cognitive representation of the context encoded at the hippocampus. The hippocampus is an essential brain area for the memory process. Particularly, its role in spatial memory, its neuronal representation of the context, and its relationship with spatial memory, has been extensively studied since the discovery of hippocampal place cells [7]. These neurons are active when the animal goes through a certain location in a given context and different contexts will be represented by distinct population of active place cells [8]. While place cells activity appears to depend on the environment, the LFP seems to be invariant for any location, environment, or context.

In this work, we apply DMD to obtain a dynamical representation of the systems underlying the LFP recorded in the CA1 region of the hippocampus in rats exploring different contexts. To test the hypothesis that the hippocampal representation of the context could be read from the LFP, the obtained systems were subject to a classification task. If the dynamical representation obtained from the LFPs, recorded in a given environment is characteristic of that environment, a classifier should be able to infer the context from the LFP. The motivation for this work is two-fold. In the first place, to extract information from a complex signal such as the hippocampal LFP remains an open question, although some advances have been made, in particular, for position encoding, by applying static methods such as ICA [9]. Secondly, the study of population signals, such as LFPs, involves a recording process that is more robust to adverse experimental conditions than recording single cell activity, such as place cells. Thus if complex brain representation could be extracted from LFPs, it would be a better approach to brain-machine interfaces for human patients.

The present work is a consequence of previous research by the authors in García-Violini et al. [10], Bertone-Cueto et al. [11]. The experimental data has been presented here for the first time.

The remainder of this paper is organized as follows. In Section 2 the general context classification methodology is described. Particularly, the basics of the DMD method are recalled in Section 2.1 while in Section 2.2 the clustering methodology employed in this study, for the classification of the results obtained with DMD, is described. Section 3 details the experimental setup which includes both the biological parts and the signal acquisition platforms. The results obtained here are discussed in Section 4. Finally, conclusions on the overall application of the proposed methodology are provided in Section 5.

2. Classification approach

In this section, the classification approach used for the context characterization is described. The interested reader is referred to Kutz et al. [12] and Zheng et al. [13] for a detailed discussion about these methods. A graphical scheme is presented in the center and right part of Fig. 1.

2.1. Dynamic mode decomposition

The goal of DMD is to describe the measured states with empirically computed vectors, or "dynamic modes", extracted directly from data [12]. Thus, patterns that represent spatial correlation modes are associated with a specific linear dynamic behavior, which may be, fixed-frequency oscillatory and/or be combined with exponential decay or growth. For the application of the method, a fixed-sampling rate with Zero-Order Hold (ZOH) is used, i.e., the measured voltages $\mathbf{x}$ are sampled at times t_k, with $k = 1, 2, 3, \ldots, m$. Then, a regression is performed on the linear dynamical system $\mathbf{x}_{k+1} = \mathbf{A}\mathbf{x}_k$, choosing $\mathbf{A}$ such that $\|\mathbf{x}_{k+1} - \mathbf{A}\mathbf{x}_k\|_2$, is minimized over the $k = 1, 2, 3, \ldots, m-1$ samples. Therefore, the state-matrix $\mathbf{A}$, represents the best (finite) linear operator that advances the states from k to $k+1$, over the chosen time window. In most cases of practical interest, the assumption of linearity $\mathbf{x}_{k+1} = \mathbf{A}\mathbf{x}_k$, is satisfied approximately within certain bounds. For the cases where this approach fails, there exist extensions of the standard method. Specifically, the extension used in this work, employs time-lagged samples or delay coordinates, in order to include historical information of the system. This is particularly useful for complex systems with periodic or quasi-periodic behavior [14], and also, when the relevant number of states (n) and time samples (m) are unbalanced, e.g., like in the case of this study ($n = 15$ and $m = 300$). This approach constitutes a generalization of the standard method and is implemented, for example, in Higher Order Dynamic Mode Decomposition (HODMD) [15], where its goal is to yield a more general expansion than that obtained by DMD. This is possible due to the following higher order Koopman assumption [15]:

$$\mathbf{x}_{k+s} = \mathbf{A}_1\mathbf{x}_k + \mathbf{A}_2\mathbf{x}_{k+1} + \ldots + \mathbf{A}_s\mathbf{x}_{k+s-1}, \tag{1}$$

with $k = 1, \ldots, m-s$ and s, a tunable parameter. This relation can be reformulated as:

$$\tilde{\mathbf{x}}_{k+1} = \tilde{\mathbf{A}}\tilde{\mathbf{x}}_k, \tag{2}$$

where the augmented state vectors and the augmented Koopman matrix are explicitly:

$$\begin{bmatrix} \mathbf{x}_{k+1} \\ \mathbf{x}_{k+2} \\ \ldots \\ \mathbf{x}_{k+s-1} \\ \mathbf{x}_{k+s} \end{bmatrix} = \begin{bmatrix} \mathbf{0} & \mathbf{I} & \mathbf{0} & \ldots & \mathbf{0} & \mathbf{0} \\ \mathbf{0} & \mathbf{0} & \mathbf{I} & \ldots & \mathbf{0} & \mathbf{0} \\ \ldots & \ldots & \ldots & \ldots & \ldots & \ldots \\ \mathbf{0} & \mathbf{0} & \mathbf{0} & \ldots & \mathbf{0} & \mathbf{I} \\ \mathbf{A}_1 & \mathbf{A}_2 & \mathbf{A}_3 & \ldots & \mathbf{A}_{s-1} & \mathbf{A}_s \end{bmatrix} \begin{bmatrix} \mathbf{x}_k \\ \mathbf{x}_{k+1} \\ \ldots \\ \mathbf{x}_{k+s-2} \\ \mathbf{x}_{k+s-1} \end{bmatrix}, \tag{3}$$

with $\mathbf{I}$ and $\mathbf{0}$, the $n \times n$ identity matrix and $n \times n$ zero matrix, respectively. In this way, HODMD is performed by applying DMD to the augmented samples given by (3). Using delay coordinates, the data matrices are augmented by stacking (hence the s parameter

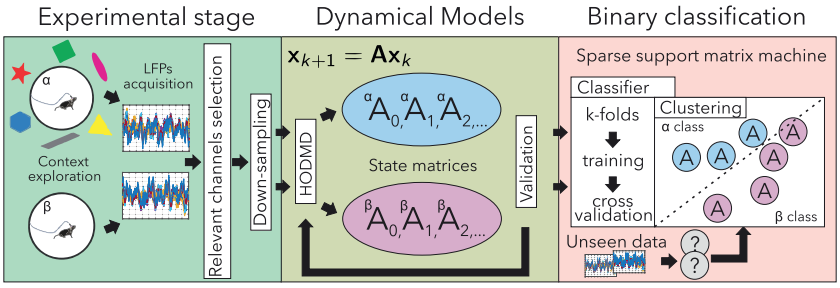

Fig. 1. Left: The signals of interest (LFPs) are acquired during the different behavioral tasks. The raw data is pre-processed. Center: Linear time-invariant state space models are obtained by applying the HODMD method to each set of signals, over the chosen time window. Right: The classifier is trained with the state matrices corresponding to each context, then, the binary clustering of the predictors is performed.

name) the shifted state vectors in the block-Hankel form:

$$\mathbf{X}_{\text{au}} = \begin{bmatrix} \mathbf{x}_1 & \mathbf{x}_2 & \dots & \mathbf{x}_{m-s} \\ \mathbf{x}_2 & \mathbf{x}_3 & \dots & \mathbf{x}_{m-s+1} \\ \vdots & \vdots & \ddots & \vdots \\ \mathbf{x}_s & \mathbf{x}_{s+1} & \dots & \mathbf{x}_{m-1} \end{bmatrix}, \tag{4}$$

$$\mathbf{X}'_{\text{au}} = \begin{bmatrix} \mathbf{x}_2 & \mathbf{x}_3 & \dots & \mathbf{x}_{m-s+1} \\ \mathbf{x}_3 & \mathbf{x}_4 & \dots & \mathbf{x}_{m-s+2} \\ \vdots & \vdots & \ddots & \vdots \\ \mathbf{x}_{s+1} & \mathbf{x}_{s+2} & \dots & \mathbf{x}_m \end{bmatrix}. \tag{5}$$

Then, a regression is performed to obtain the augmented state matrix for each set of signals, i.e.:

$$\tilde{\mathbf{A}}_i = \mathbf{X}'_{\text{au}} \mathbf{X}^{\dagger}_{\text{au}}, \tag{6}$$

where † denotes the Moore–Penrose pseudo-inverse, and i, the window number. The validation of this stage takes into account the model outputs versus the measured voltages, such that, the absolute error is bounded.

2.2. Context classification and clustering

In order to serve as predictors, the obtained matrices should represent a distinctive characteristic for each context. Unlike common cases where the predictors are in scalar or vector-form, dealing with matrices carry an issue: a typical approach is to reshape the matrices for further classification, losing the intrinsic structural information in the process [16].

Given this difficulty, the binary matrix classifier, Sparse Support Matrix Machine (SSMM) [13] was chosen. It should be noted that the state matrices show a clear structure, as depicted in (3), that is not context-dependent but rather due to the HODMD method itself. The SSMM method uses a hinge-loss function to train the classifiers under the large-margin principle, including a regularization process on the regression matrix, in order to prevent over-fitting. Let $\{\tilde{\mathbf{A}}_i, y_i\}$ be a training set of samples, where $\tilde{\mathbf{A}}_i \in \mathbb{R}^{sn \times sn}$ is the ith input matrix and $y_i \in \{1, -1\}$ its corresponding class (true label). A $f : \mathbb{R}^{sn \times sn} \to \mathbb{R}$ function was trained to identify new data category by optimizing the following objective function:

$$\arg\min_{\mathbf{W},b} \gamma \|\mathbf{W}\|_1 + \tau \|\mathbf{W}\|_* + \sum_{i=1}^{k} \{1 - y_i[tr(\mathbf{W}^T \tilde{\mathbf{A}}_i) + b]\}_+,$$

where, $\mathbf{W}$ is the regression matrix, b and offset term, $\{1-u\}_+ = \max(0, 1-u)$ denotes the hinge-loss function, and $\|\mathbf{W}\|_1 = \sum_{i,j} |w_{i,j}|$ and $\|\mathbf{W}\|_* = \sum_{i=1}^{r} \sigma_i$ are the ℓ_1-norm and nuclear norm, respectively. The restrictions imposed via linear combination of these two norms, and weighted by γ and τ respectively, promote two characteristics: the sparsity property, which removes redundant information retaining explanatory features, and the low-rank property, which is used to capture the correlation within matrices, regulating the classifier complexity. These parameters were empirically tuned to achieve high precision in the primary $\alpha - \beta$ classification, as shown in Section 4.

In order to estimate the classification error, a cross-validation scheme was implemented using the k-folds method [17]. This method roughly consists in using a fraction of the data to fit the model (in this case, the classifier), reserving a different part to test its performance. The available data is partitioned in k sets, using $k-1$ to train, and leaving one out to validate. It is important to note, that the use of random indices to choose the partitions, should mitigate, in a sense, the effect of time-variability of the underlying dynamical systems. All tests were performed using $k = 10$ folds, choice that generally performs well in terms of the bias-variance trade-off [18], and $i = 25$, number of windows for each set of signals (coming from 15 electrodes) that represent 6 s worth of the recorded LFPs. This amount of data was determined focusing on the balance between classification performance, as well as training time.

The classification success and error cases are defined as: True Positives (TP), the classifier assigns α class to samples obtained from signals acquired in the α context. False Positives (FP), the classifier assigns α class to samples obtained from signals acquired in the β context. False Negatives (FN), the classifier assigns β class to samples obtained from signals acquired in the α context. And finally, True Negatives (TN): the classifier assigns β class to samples obtained from signals acquired in the β context. For the assessment of the classifiers, three metrics are used. The sensitivity metric, represents the rate of real positives detected, and the specificity metric, represents the rate of real negatives detected:

$$\text{Sensitivity} = \frac{TP}{TP+FN}, \quad \text{Specificity} = \frac{TN}{TN+FP}.$$

The Matthew's Correlation Coefficient (MCC), considers all the cases of success and error in the formula:

$$\text{MCC} = \frac{TP \times TN - FP \times FN}{\sqrt{(TP+FP)(TP+FN)(TN+FP)(TN+FN)}}.$$

Analogously to the correlation coefficient, its possible values lie in $[-1\ 1]$, having an easy interpretation. A MMC $= 1$ means a perfect classifier, and MMC $= -1$, an always-wrong one. A graphical illustration of this process in depicted in Fig. 1 right.

3. Material and methods

3.1. Experimental stage: data collecting

This section is illustrated by the left part of Fig. 1. Electrophysiological data were acquired while rats were exploring an open field. The open field consists of an open arena, 1 meter in diameter with surrounding walls (30 cm tall). On a particular day,

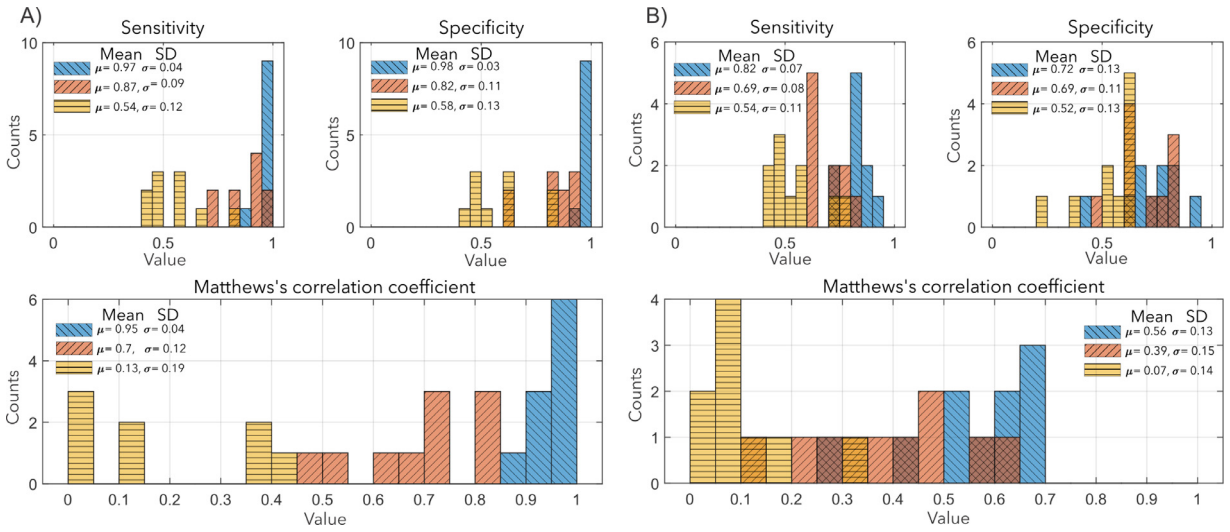

Fig. 2. Classification - The histograms of the metrics computed to assess the performance along the 10 folds are shown, for both rats A and B, as indicated in the left-right panels, respectively. The legend entries indicate, both mean and standard deviation for the α vs. β, the α vs. α', and the α vs. α tasks comparison respectively. The y-label, in all the histograms, shows the counts, to indicate the number of occurrences in each bin.

animals were exposed to the open field twice, separated by four hours. In the first visit to the open field six external cues were visible (context α). After four hours, in the second visit, the animal could be exposed to exactly the same context (the same open field with the same 6 clues, context α') or to the same open field without any external cues, (context β). Each visit to the open field lasted 15 min. For this study, data was collected from 2 animals. Experiments were carried out on Long Evans rats implanted with 15 tetrodes (4 12-μm tungsten wires twisted together) in the hippocampal CA1 brain region. For further analysis, only one channel per tetrode was selected, such that there were no information redundancy. The signal was acquired at 20 kHz sample rate (Amplipex LTD, Hungary). For the application of the algorithms, the signal was down-sampled to 1.25 kHz allowing faster computation and a reduced dataset storage.

3.2. Data analysis

The method chosen to obtain the dynamical models was HODMD. This method was applied to sequential time windows for each set of signals, according to the following criterion: the time length of 240 ms ($m = 300$ data points @ 1.25 kHz) manages to cover approximately two cycles of the dominant θ rhythm present in the signals, being short enough to consider that the underlying system remains time-invariant along each window. From this trade-off, the LFPs time series were modeled with successive Linear Time-Invariant (LTI) state-space representations in a linear piece-wise manner. Within the several ways to compute the state matrix **A**, the Moore–Penrose pseudo-inverse was chosen, for two main reasons. First, according to the proposed hypothesis of context characterization based on the exhibited dynamics, this method retains as much detail as possible on the outputs of the system (see [12] for further details). At this point, if an order reduction would have been applied, it could have removed the characteristic modes in which the difference between contexts emerge. This is because, those modes could be very significant from the biological process standpoint, but they may not contribute in the same way to the output energy, falling below some truncation threshold in a reduction approach. Although there is no direct biological interpretation of the obtained modes, the association between them and the neural processes will be further studied by the authors, since it could constitute a useful tool for analysis. Secondly, the models obtained via pseudo-inverse are tractable, both in computation time as in analysis and visualization. The DMD method was first developed to study complex flow fields where millions of measurements can be used, and thus, a dimensionality reduction is often necessary. Instead, in neurological applications the number of available electrodes, or recording locations, range from tens to hundreds, while the number of acquired data points could scale up to thousands depending on the application.

A spectral analysis of the matrices obtained in each context was performed, in which, the distribution of its lightly-damped eigenvalues did not establish any clear difference between them. Furthermore, preliminary approaches such as Support Vector Machines (SVM), decision trees and nearest neighbors were used in order to separate these sets without success. This proved to be a non-trivial classification problem which led to implement a more sophisticated technique, as summarized in Section 2.2.

4. Results

With the objective of proving separability using the identified dynamic matrices as predictors, a series of tests were designed. For each test, unseen data was used, i.e., data not used previously in the classifier training stage.

The first test, consisted in the comparison between the α and the β contexts. Data collected in day 2 was used in both cases. In this setting, the maximum separation was expected, since this contexts represent the unfamiliar/familiar environments, respectively. Using the k-folds method, with $k = 10$ and 25 samples for each context, an almost complete separation was achieved.

To quantify the performance of the classification along the 10 folds, histograms of the statistic metrics, sensitivity, specificity, and MCC were computed, as indicated in Fig. 2, where a striped pattern was added to the bars to bring out any superposition. The mean value of both sensitivity and specificity are very close to 1, which means, on the one hand that the test is very precise and also, that the classification is balanced since both values are comparable. The deviation σ is very small in both cases. The MCC is very close to unity, which implies that the classification scheme approaches the optimal performance.

A test that explores the effect of time variability on the recognition was also performed. In this case, the contexts were spatially the same, but the tasks were conducted at different times, i.e. with

a separation of four hours. From this distinction, the definition of the class α' arose.[1] In order to assess the classifiers, samples from context α and context α' were used. Although similar results are observed in comparison to the classification from α vs. β context, in Fig. 2 the classification from different contexts is better than for the same context at different times. This suggests that the separation due to context difference is dominant, as compared to the separation due to the time gap between exploration tasks.

Also, an α vs. α context verification was made. For this test, data coming from the same recording session was used, in order to verify that, the separation in the proposed terms, were minimal. Indeed, the obtained separation, using the same scheme of 10 folds and 25 samples per context, chosen from session subsets approximately 4 min apart, was very small. The values tending toward 0.5 for both sensibility and specificity, are equivalent to a 0.5 detection probability, which in the discrete binary case, represents the worst possible performance. This is consistent with the average MCC being near zero, indicating that the classifiers are incapable of distinguishing between classes, which was the expected outcome.

5. Conclusion

A new classification approach, applied to a biological problem, is provided in this study. Three main contributions can be highlighted. Firstly, the classification approach, which results as a combination of a DMD-based methodology with a binary matrix classifier, based on SSMM [13], is highlighted. Secondly, the application of the classification method to known/unknown contexts, is worth mentioning. Finally, the manuscript provides evidence of the context codification in LFP signals, which still is an open and key question in the area of neuroscience [20].

It is worth mentioning that, although the classification methodology is validated here in the context of a biological problem, it can be applied to a broad range of different fields, even beyond the biological scope, as mentioned in Section 3. Also, the proposed approach is based on well-known linear algebra and dynamical systems theory, and it has prove to be an efficient tool to tackle problems which are not tractable with standard identification-based methodologies, due to the intrinsic dynamical complexity of the underlying systems.

To validate the proposed methodology, a biological problem is addressed. In particular, considering that the context interpretation from LFP signals is still an open question in neuroscience (with empirical evidence [20]), the case study, presented in Section 3, is carried out using real LFPs measured in the hippocampus, in rats performing exploration tasks in an open arena with different cues.

Therefore, we have presented a proof-of-concept that it is possible to classify the context explored by an animal by analyzing the global dynamics of the CA1 hippocampal LFP. Thus, in this case study, the ability of the classification approach to distinguish when the animal visits a new context, is tested. Similar results were obtained when the animal explores the same context but at a different time. In that case, the algorithm classified them as different [19], although not as efficiently as in the context classification situation. Since the representation of a context not only involves spatial information but a more rich variety of variables it is not surprising that the dynamics of the LFP as an emergent of local computation are not the same in two situations. Thus, it is possible to consider these as two different experiences in the same context. On the other hand, the lesser separation achieved by the classifier in the same-context comparison, indicates that DMD derived LFP models detect spatial representation of the context encoded in the hippocampus more efficiently. The results show the high precision of the method and, although this is a particular biological experiment, it can be extended and adapted to a number of different applications, for example, to characterize REM and non-REM sleep cycles [21].

In addition, the results show evidence that there is a correlation between the information contained in the LFPs and the corresponding explored context. The latter will be the subject of future research by the authors. Also as a subject of future work, a statistical improvement of the results will be carried out once the circumstances of the COVID-19 pandemic, and the consequent lockdowns and restrictions globally implemented, allow the experimental laboratory work to be resumed.

[1] This phenomena was included in the fiction literature as a brain anomaly that distinguishes the same element but at two different times, as separate objects [19].

Declaration of Competing Interest

The authors declare that they have no known competing financial interests or personal relationships that could have appeared to influence the work reported in this paper.

CRediT authorship contribution statement

S. Martínez: Conceptualization, Methodology, Software, Validation, Formal analysis, Investigation, Writing - original draft. **A. Silva:** Investigation, Resources. **D. García-Violini:** Conceptualization, Investigation, Writing - review & editing, Supervision. **J. Piriz:** Conceptualization, Investigation, Resources, Writing - review & editing, Funding acquisition. **M. Belluscio:** Conceptualization, Investigation, Resources, Writing - review & editing, Funding acquisition. **R. Sánchez-Peña:** Conceptualization, Methodology, Investigation, Writing - review & editing, Supervision, Project administration, Funding acquisition.

Acknowledgment

The authors are financed by a PICT2017-2417 Grant from ANPCyT (MinCTeI), Argentina.

References

[1] Papoulis A. Probability, random variables, and stochastic processes. 2nd ed. McGraw-Hill; 1984.
[2] Ljung L. System identification: theory for the user. Upper Saddle River, NJ: PTR Prentice Hall; 1999. p. 1–14.
[3] Kutz JN, Brunton SL, Brunton BW, Proctor JL. Dynamic mode decomposition: data-driven modeling of complex systems. SIAM; 2016.
[4] Buzsáki G, Draguhn A. Neuronal oscillations in cortical networks. science 2004;304(5679):1926–9.
[5] Brunton B, Johnson L, Ojemann J, Kutz J. Extracting spatial-temporal coherent patterns in large-scale neural recordings using dynamic mode decomposition. J Neurosci Methods 2014;258.
[6] Solaija MS, Saleem S, Khurshid K, Hassan S, Kamboh A. Dynamic mode decomposition based epileptic seizure detection from scalp EEG. IEEE Access 2018.
[7] O'Keefe J, Dostrovsky J. The hippocampus as a spatial map: preliminary evidence from unit activity in the freely-moving rat.. Brain Res 1971.
[8] Muller RU, Kubie JL. The effects of changes in the environment on the spatial firing of hippocampal complex-spike cells. J Neurosci 1987;7(7):1951–68.
[9] Agarwal G, Stevenson IH, Berényi A, Mizuseki K, Buzsáki G, Sommer FT. Spatially distributed local fields in the hippocampus encode rat position. Science 2014;344(6184):626–30.
[10] García-Violini D, Bertone NI, Martínez S, Chiesa-Docampo F, De la Fuente V, Belluscio M, et al. Closed-loop in neuroscience: can a brain be controlled?. In: 2018 Argentine conference on automatic control (AADECA); 2018. p. 1–6. doi:10.23919/AADECA.2018.8577350.
[11] Bertone-Cueto NI, Makarova J, Mosqueira A, García-Violini D, Sánchez-Peña R, Herreras O, Belluscio M, Piriz J. Volume-conducted origin of the field potential at the lateral habenula. Front Syst Neurosci 2020;13:78.
[12] Kutz JN, Brunton SL, Luchtenburg DM, Rowley CW, Tu JH. On dynamic mode decomposition: Theory and applications. J Comput Dyn 2014;1(2):391–421.
[13] Zheng Q, Zhu F, Qin J, Chen B, Heng P-A. Sparse support matrix machine. Pattern Recognit 2018;76(C):715–26.
[14] Takens F. Detecting strange attractors in turbulence. In: Rand D, Young L-S, editors. Dynamical systems and turbulence, Warwick 1980. Berlin, Heidelberg: Springer Berlin Heidelberg; 1981. p. 366–81. ISBN 978-3-540-38945-3.

[15] Le Clainche S, Vega J. Higher order dynamic mode decomposition. SIAM J Appl Dyn Syst 2017;16:882–925.
[16] Luo L, Xie Y, Zhang Z, Li W-J. Support matrix machines. In: Bach F, Blei D, editors. Proceedings of the 32nd international conference on machine learning. Proceedings of Machine Learning Research, 37. Lille, France: PMLR; 2015. p. 938–47.
[17] Friedman J, Hastie T, Tibshirani R. The elements of statistical learning, 1. Springer Series in Statistics New York; 2001.
[18] Breiman L, Spector P. Submodel selection and evaluation in regression. The x-random case. Int Stat Rev 1992;60(3):291–319.
[19] Borges JL. Funes el memorioso (Ficciones). Buenos Aires: Emecé Editores; 1944.
[20] Smith DM, Mizumori SJ. Learning-related development of context-specific neuronal responses to places and events: the hippocampal role in context processing. J Neurosci 2006;26(12):3154–63.
[21] Moris E, Forcato C, Larrabide I. Supervised learning for sleep stage scoring using random forest: Is a simpler model accurate enough on unseen individuals?. In: 2021 IEEE international conference on acoustics, speech and signal processing. IEEE; 2021. Submitted